On the Performance Evaluation of Pan-Sharpening Techniques

Qian Du, *Senior Member, IEEE*, Nicholas H. Younan, *Senior Member, IEEE*, Roger King, *Senior Member, IEEE*, and Vijay P. Shah, *Student Member, IEEE*

***Abstract*—The limitations of the currently existing pan-sharpening quality indices are analyzed: the absolute difference between pixel values, mean shifting, and dynamic range change is frequently used as spatial fidelity measurement, but they may not correlate well with the actual change of image content; and spectral angle is a widely used metric for spectral fidelity, but the spectral angle remains the same if two vectors are multiplied by two individual constants, which means the average spectral angle between two multispectal images is zero even if pixel vectors are multiplied by different constants. Therefore, it is important to evaluate the quality of a pan-sharpened image under a task of its practical use and to assess spectral fidelity in the context of an image. In this letter, three data analysis techniques in linear unmixing, detection, and classification are applied to evaluate spectral information within a spatial scene context. It is demonstrated that those old but simplest approaches, i.e., Brovey and multiplicative (or after straightforward adjustment) methods, can generally yield acceptable data analysis results. Thus, it is necessary to consider the tradeoff between computational complexity, actual improvement on application, and hardware implementation when developing a pan-sharpening method.**

***Index Terms*—Classification, detection, linear unmixing, multispectral (MS) image, pan sharpening, performance evaluation.**

I. Introduction

PAN SHARPENING is a typical approach to integrating the spatial details of a high-resolution panchromatic (pan) image and the spectral information of a low-resolution multispectral (MS) image to produce a high-resolution MS image. Many pan-sharpening methods have been developed [1], [2], [7]. The major pan-sharpening methods are reviewed below.

Intensity–Hue–Saturation (IHS) Transform-Based Methods: Three bands of an MS image are considered as three components in a color image. An IHS transform is conducted, which separates the intensity from the two color components. The pan image replaces the intensity component. Then, a pan-sharpened image can be generated via the inverse IHS transform [3]. The drawback of this method is that it is only suitable to a three-band MS image. Tu *et al.* proposed a generalized approach that can apply the IHS-based pan sharpening to four-band MS images [4]. However, its performance relies on the choice of an empirical data-specific parameter controlling the contributions of blue and green bands to the fused image, and the near infrared band is prone to be distorted.

Manuscript received September 1, 2006; revised February 23, 2007.

The authors are with the Department of Electrical and Computer Engineering, and the GeoResources Institute (GRI), High Performance Computing Collaboratory, Mississippi State University, Mississippi State, MS 39762 USA.

Digital Object Identifier 10.1109/LGRS.2007.896328

Principal Component Analysis (PCA)-Based Methods: PCA is another commonly used technique. PCA is applied to the original image. Then, the first principal component (PC) image is replaced by the pan image [5]. Here, it is assumed that the first PC image with the largest variance contains the major information in the original image. However, it is known that data information is distributed among several PCs. So obviously, this method brings about spectral distortion.

Brovey Method: In the Brovey method, the ith band is sharpened by Fused Band $i = K * \text{Pan} * \text{Band } i/(\text{Band } 1 + \text{Band } 2 + \cdots + \text{Band } K)$, where K is the number of bands in an MS image [6]. The computation is on the pixel-by-pixel base. The angle from the Spectral Angle Mapper (SAM) between the original (after up-sampling) and pan-sharpened MS images is 0°. This is because the operation of multiplication only changes the norm of a spectral vector.

Multiplicative Method: It is similar to the Brovey method [7]. The only difference is that the multiplication result is not normalized, i.e., Fused Band $i = \text{Pan} * \text{Band } i$. As in the Brovey method, the SAM value between the original (after up-sampling) and pan-sharpened MS images is 0°. Due to the lack of normalization term, the dynamic range of pixel values is significantly changed.

Wavelet-Based Methods: A wavelet-based method includes three steps: forward transform; coefficient combination; and backward transform. Many different ways are proposed to fuse the wavelet coefficients of the original MS image and the pan image. It remains as the most active research area.

In addition, a technique based on Gram–Schmidt (GS) orthogonalization in the ENVI package is well known [8]; and Zhang's approach that utilizes the least squares technique to adjust the contribution of individual MS bands to the fusion result is available in the PCI Geomatica software [1].

It is necessary to quantitatively evaluate the performance of these methods [9]–[11]. Current performance evaluation is mainly focused on absolute pixel value change. For instance, frequently used metrics for spatial similarity are the mean squared error (MSE), root mean squared error (RMSE), etc. When spatial resolution is improved, it is still necessary to evaluate the spectral fidelity. The SAM is frequently used to compare the spectral similarity pixel-by-pixel. Another way to qualitatively evaluate the spectral fidelity is to display a three-band color combination using the original and pan-sharpened MS image and compare the color tone [1]. In our research, we evaluate the quality of a pan-sharpened image under a task of its practical use. In other words, we focus on its performance in the following data analysis. In this way, the spatial and spectral quality of the fused image can be jointly evaluated.

In this letter, the PCA, Brovey, multiplicative, GS, and Zhang's methods are selected for evaluation due to their maturity and easy access in commercial software.

II. Quantitative Evaluation Metrics

A. Review of Quality Indices

Quantitative evaluation of pan-sharpened images has been investigated since this technique was developed [9]–[11]. One focus is the spatial fidelity, i.e., comparing the spatial similarity of a band before and after sharpening. Another focus is the spectral fidelity, i.e., comparing the spectral similarity of a pixel vector before and after sharpening. The frequently used quality metrics are reviewed as below.

MSE and RMSE: MSE and RMSE are frequently used to compare the difference between the original and pan-sharpened MS images by directly calculating the changes in pixel values [12].

SAM (θ): SAM is widely used in measuring spectral fidelity [13]. It calculates the angle between two pixel vectors. If the angle is 0°, this means no spectral change. It is performed on a pixel-by-pixel base.

Correlation Coefficient (ρ): The correlation coefficient is the most popular similarity metric in measuring spatial fidelity [10]. A value close to one means that two images are similar. It is insensitive to mean shifting and the change of dynamic range after mean removal and variance normalization.

Relative Dimensionless Global Error in Synthesis (ERGAS): The ERGAS value is defined as [14]

$$\text{ERGAS} = 100\frac{h}{l}\sqrt{\frac{1}{K}\sum_{k=1}^{K}\left(\frac{\text{RMSE}(k)}{\mu(k)}\right)^2} \tag{1}$$

where h/l is the ratio between pixel sizes of pan and original MS images, and $\text{RMSE}(k)$ and $\mu(k)$ are the RMSE and mean of the kth band, respectively. It considers sensor specification. A small ERGAS means good image quality. It is sensitive to mean shifting and dynamic range change.

Universal Image Quality Index (Q): The difference between image A and B can be quantified as

$$Q = \frac{\sigma_{AB}}{\sigma_A\sigma_B}\cdot\frac{2\mu_A\mu_B}{\mu_A^2+\mu_B^2}\cdot\frac{2\sigma_A\sigma_B}{\sigma_A^2+\sigma_B^2} \tag{2}$$

where σ_A and σ_B are the standard deviations of image A and B, respectively. In (2), the first term is the correlation coefficient, the second term is about mean shifting, and the third term is about contrast similarity [15]. A Q value close to one means good quality.

Quaternions Theory Based Quality Index ($Q4$): The Q index can be generalized to Q_4 for a four-band MS image using the theory of quaternions. Then, the comparison can be conducted on the entire MS image instead of one band after another. Detailed development can be found in [16].

B. Limitations of Existing Quality Indices

When comparing a pixel value spatially, it is known that any mean shifting and dynamic range change can lead to large MSE and RMSE. However, this does not mean the image content is greatly changed. For instance, if all the pixel values in a band are increased or decreased by a constant (mean shifting) or multiplied by a constant (variance and dynamic range change), the content in this band image is not actually changed. In addition to MSE and RMSE, the aforementioned ERGAS, Q, and Q_4 suffer the same problem because they all include the components related to RMSE, mean shifting, or contrast change. Therefore, unless the fused image will be compared with a predefined spatial or spectral pattern requiring precise matching in pixel value in the following data analysis step, these metrics may not be well correlated with the data analysis performance. On the other hand, a fused image considered to have poor quality using these metrics may have acceptable data analysis result as long as the image content is well preserved.

For an MS image, spectral information is particularly important when the spatial resolution is rough. SAM can be used for spectrally comparing a pixel vector. When a pixel vector is multiplied by a constant, the change in SAM is 0° because the vector is basically not changed except the norm. When pixel vectors in an MS image are multiplied by values varied from pixel to pixel, as in the Brovey and multiplicative methods, the average SAM is still 0°, but each band image is greatly changed due to different values being involved in the multiplication from pixel to pixel. Therefore, it is important to jointly evaluate the spectral fidelity of pixels in the context of an image instead of treating them separately.

This letter is focused on image content change and its impact on practical applications. In particular, spectral-analysis-based techniques are employed for the evaluation. These techniques explore spectral information to fulfill a certain purpose, which are described in Section III.

III. Application-Oriented Performance Evaluation

The three data analysis techniques for evaluation are linear unmixing, detection, and classification. The spectral information in an MS image within the context of an image scene is used in these spectral-analysis-based techniques, so the spectral and spatial fidelity of the pan-sharpened MS image can be jointly evaluated. Because it is difficult to have prior information about the various image scenes involved in pan sharpening for evaluation, unsupervised methods are applied first. The results from the original MS image are considered as the ground truth. The extracted endmember or class signatures can be used to conduct supervised evaluation.

A. Linear Unmixing

Linear mixture analysis is often used to analyze mixed pixel composition. According to the linear mixture model, a pixel value can be considered as the linear mixture from the distinctive endmember signatures present in an image scene. The endmember signatures and their abundances are estimated from the original and pan-sharpened images. This can be accomplished by applying the unsupervised fully constrained least squares linear unmixing (UFCLSLU) algorithm [17]. Then, the two corresponding endmember signatures from the original and pan-sharpened images are compared to evaluate the spectral information distortion, while two corresponding abundance

images are compared to evaluate the spatial similarity. The number of endmembers that can be extracted is equal to the number of spectral bands when dealing with multispectral imagery.

The endmembers extracted from the original MS image with UFCLSLU can be used to conduct the supervised FCLSLU for the fused image [17]. The resulting abundance images are compared with those from the original MS image.

B. Detection

Target detection is another important application of remote sensing data. When no target information is available, an unsupervised detection technique is applied, which actually performs anomaly detection. An anomaly is defined as a small object whose spectral signature is very different from the background, which is most likely an unknown target. Anomaly detection is a good technique to test the performance of a pan-sharpening method in detailed information preservation, because these small objects are prone to be sacrificed. The well-known RX algorithm is adopted for this purpose [18]. Since there is no ground truth available, the detection map using the original data is considered as the ground truth, and the detection map using the pan-sharpened data is compared with it. The metric of similarity comparison is the spatial correlation coefficient.

To evaluate the supervised detection performance, the most anomalous pixel from the anomaly detection map using the RX algorithm is chosen as the target signature. Then, the constrained energy minimization (CEM) algorithm is applied to the original and fused MS images [19] followed by the similarity comparison of detection maps.

C. Classification

Independent component analysis (ICA) is a popular technique for unsupervised classification when no prior class information is available. Its basic idea is to decompose a set of multivariate signals into the basis of statistically independent sources with minimal loss of information content so as to achieve classification. The well-known FastICA algorithm can be used for this purpose [20]. For a four-band MS image, there are four classification maps to be generated. When no ground truth is available, the classification maps using the original data are considered as the ground truth, and the classification maps using the pan-sharpened data are compared with them. The correlation coefficient is employed to compare the similarity.

IV. Experiments

Four-band IKONOS and QuickBird data were used in the experiments. Both the pan and the original MS were degraded before pan sharpening such that the pan-sharpened MS image has the same size as the original MS image. Then, the pan-sharpened MS image was compared with the original MS image. The frequently used quality indices such as correlation coefficient (ρ), SAM (θ), ERGAS, Q, and $Q4$ were employed. The three data analysis techniques in Section III, i.e., UFCLSLU and FCLSLU for linear unmixing, RX and CEM algorithm for detection, and FastICA for classification, were applied to evaluate the performance of pan-sharpened methods in practical applications.

(a) (b)

Fig. 1. IKONOS image scene used in the experiment. (a) Degraded pan image. (b) Original MS image (Band 3).

TABLE I
Traditional Performance Evaluation for the IKONOS Image Scene

	ρ_{avg}	θ_{avg}	ERGAS	Q_{avg}	Q_4
PCA	0.7872	11.1701	7.3282	0.7204	0.7928
Brovey	0.8738	4.7811	5.2215	0.8160	0.8238
Multiplicative	0.8456	4.7814	30.1095	0.0001	0.0001
Multiplicative*	0.8456	4.7814	10.1271	0.7072	0.7168
GS	0.7937	6.3943	6.0319	0.7682	0.7870
Zhang	0.8916	5.4310	4.2466	0.8733	0.8824

A. IKONOS Example

A small subimage about an urban area of size 256×256 was used. The 1-m pan after degradation and 4-m original MS images are shown in Fig. 1.

The correlation coefficients ρ_{avg} are listed in Table I, which shows the averaged values of the four spectral bands before and after sharpening. SAM values θ_{avg} are also listed in Table I, which shows the averages from all pixel vectors. We can see that the Brovey and multiplicative methods performed very well in terms of yielding larger ρ_{avg} and smaller θ_{avg}. However, the multiplicative method produced very large ERGAS and very low Q_{avg} and Q_4 because of great changes in the mean and dynamic range.

However, the mean shifting and dynamic range change can be easily adjusted without changing the image content. For the multiplicative method, the adjustment can be achieved by dividing the mean of the pan image, i.e.,

$$\text{Multiplicative}^* = \frac{\text{Multiplicative}}{\mu(\text{Pan})}. \tag{3}$$

In Table I, we can see that after such a simple adjustment, ERGAS was greatly decreased, while Q_{avg} and Q_4 were greatly increased. It is noteworthy that ρ_{avg} and θ_{avg} were not changed. The fused image was just divided by a constant, but ERGAS, Q_{avg}, and Q_4 were significantly different. This means that these changes may not be well correlated with the image content.

Table II lists the performance evaluation results when applying linear unmixing to the original and pan-sharpened MS images, where $\bar{\rho}_{\text{avg}}$ denotes the averaged correlation coefficients between the four pairs of abundance images, and $\bar{\theta}_{\text{avg}}$ denotes the averaged SAM between four pairs of endmember signatures from UFCLSLU. The endmember signatures from

TABLE II
PERFORMANCE EVALUATION USING UNSUPERVISED (UFCLSLU) AND SUPERVISED (FCLSLU) LINEAR UNMIXING FOR THE IKONOS IMAGE SCENE

	$\overline{\rho}_{avg}$	$\overline{\theta}_{avg}$	$\overline{\rho}^{s}_{avg}$
PCA	0.5133	14.7453	0.6809
Brovey	0.6541	6.3802	0.7517
Multiplicative	0.6405	8.7512	0.1981
Multiplicative*	0.6405	8.7512	0.7655
GS	0.4455	14.4599	0.7673
Zhang	0.4762	14.7998	0.8206

TABLE III
PERFORMANCE EVALUATION USING UNSUPERVISED (RX) AND SUPERVISED (CEM) TARGET DETECTION FOR THE IKONOS IMAGE SCENE

	$\hat{\rho}$	$\hat{\rho}^{s}$
PCA	0.8447	0.7526
Brovey	0.8154	0.7781
Multiplicative	0.7368	0.7637
Multiplicative*	0.7368	0.7637
GS	0.8224	0.7426
Zhang	0.8239	0.7257

TABLE IV
PERFORMANCE EVALUATION USING UNSUPERVISED CLASSIFICATION (FASTICA) FOR THE IKONOS IMAGE SCENE

	$\widetilde{\rho}_{avg}$
PCA	0.7942
Brovey	0.7483
Multiplicative	0.7839
Multiplicative*	0.7839
GS	0.7858
Zhang	0.7962

the original MS image were used to apply the supervised FCLSLU analysis on the fused images, and $\bar{\rho}^{s}_{\text{avg}}$ denotes the similarity between the corresponding abundance images. The Brovey method generated the best result of UFCLSLU both spatially and spectrally. Zhang's method provided the best FCLSLU result. Interestingly, the adjusted multiplicative method yielded good results supervised and unsupervised. It should be noted that the supervised FCLSLU has difficulty in applying to the fused image from the original multiplicative method. This is because the abundance sum-to-one constraint cannot be satisfied due to the great changes of pixel values.

Table III lists the correlation coefficient $\hat{\rho}$ between the detection maps from the original and pan-sharpened images using the RX algorithm and $\hat{\rho}^{s}$ using the supervised CEM algorithm with the desired target signature being chosen as the most anomalous pixels in the RX detection map from the original MS image. Table IV shows the averaged correlation coefficient $\tilde{\rho}_{\text{avg}}$ between the classification maps from the original and pan-sharpened images using the FastICA algorithm. All these methods generated comparable results. It should be noted that the performance of the multiplicative method before and after adjustment was not changed, which means that the mean shifting and dynamic range change do not affect target detection and classification in this case.

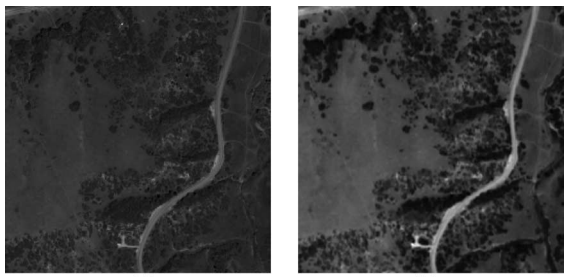

(a) (b)

Fig. 2. QuickBird image scene used in the experiment. (a) Degraded pan image. (b) Original MS image (Band 3).

TABLE V
TRADITIONAL PERFORMANCE EVALUATION FOR THE QUICKBIRD IMAGE SCENE

	ρ_{avg}	θ_{avg}	ERGAS	Q_{avg}	Q_4
PCA	0.8410	4.3513	5.7326	0.6115	0.6185
Brovey	0.8965	2.3889	3.1997	0.8748	0.8920
Multiplicative	0.8478	2.3896	26.1022	0.0001	0.0001
Multiplicative*	0.8478	2.3896	4.3747	0.7319	0.7644
GS	0.9094	2.3171	1.9680	0.8953	0.9030
Zhang	0.9216	2.1221	1.8163	0.9090	0.9168

TABLE VI
PERFORMANCE EVALUATION USING UNSUPERVISED (UFCLSLU) AND SUPERVISED (FCLSLU) LINEAR UNMIXING FOR THE QUICKBIRD IMAGE SCENE

	$\overline{\rho}_{avg}$	$\overline{\theta}_{avg}$	$\overline{\rho}^{s}_{avg}$
PCA	0.4320	9.3215	0.7787
Brovey	0.7270	6.3748	0.7534
Multiplicative	0.7606	7.2141	0.1387
Multiplicative*	0.7606	7.2141	0.7311
GS	0.7301	21.2904	0.8706
Zhang	0.5949	12.5297	0.8956

B. QuickBird Example

A small subimage about a mountainous area of size 256 × 256 was used. The 0.7-m pan after degradation and 2.8-m original MS images are shown in Fig. 2.

Table V lists the five quality measurement results. The five pan-sharpening methods provided similar ρ_{avg}. The results from the Brovey and multiplicative methods included very little spectral distortion at the pixel level, so θ_{avg} were very small as expected. The multiplicative method produced very large ERGAS and very low Q_{avg} and Q_4. After the adjustment using (3), ERGAS was greatly decreased, while Q_{avg} and Q_4 were greatly increased.

Tables VI–VIII list the evaluation results using linear unmixing, detection, and classification algorithms. Similar to the IKONOS experiment, the Brovey and multiplicative methods provided better results in unsupervised linear unmixing. These five methods yielded comparable results in detection and classification, while the result from Zhang's method was the best.

V. DISCUSSION AND CONCLUSION

The IKONOS and QuickBird experiments demonstrate that it may not be appropriate to directly compare the pixel value

TABLE VII
PERFORMANCE EVALUATION USING UNSUPERVISED (RX) AND SUPERVISED (CEM) TARGET DETECTION FOR THE QUICKBIRD IMAGE SCENE

	$\hat{\rho}$	$\hat{\rho}^s$
PCA	0.7370	0.6393
Brovey	0.7283	0.6831
Multiplicative	0.6990	0.6675
Multiplicative*	0.6990	0.6675
GS	0.7808	0.7092
Zhang	0.8352	0.7469

TABLE VIII
PERFORMANCE EVALUATION USING UNSUPERVISED CLASSIFICATION (FASTICA) FOR THE QUICKBIRD IMAGE SCENE

	$\widetilde{\rho}_{avg}$
PCA	0.7338
Brovey	0.6760
Multiplicative	0.6759
Multiplicative*	0.6759
GS	0.7502
Zhang	0.7775

change when evaluating the spatial fidelity of a pan-sharpening method. The frequently used spatial quality measures, such as MSE, RMSE, ERGAS, Q, and Q_4, consider the mean shifting and dynamic range change. So their results are easily influenced by simply multiplying a constant to an image, when the image actually is not really changed.

SAM is frequently used for evaluating the spectral fidelity. However, it performs the evaluation on a pixel-by-pixel base without considering the interpixel relationship. For instance, in these two experiments, the Brovey and multiplicative methods yield small SAM values. However, when applying the spectral-analysis-based algorithms, their performance is not as good as indicated by the SAM values.

In our opinion, the evaluation of a pan-sharpened image should be conducted under an application task, where we focus on the usefulness of the image data rather than its pixel value fidelity. The three applications on linear unmixing, detection, and classification explore the pixel spectral information within the spatial context of an image scene. This means that the spatial and spectral information are jointly evaluated. Based on the IKONOS and QuickBird experiments with different image scenes, we also conclude that the performance of a pan-sharpening technique may be varied with sensor and image content.

Overall, GS and Zhang's methods generated good results when being evaluated by either the application algorithms or the traditional quality indices. The Brovey method is robust in both supervised and unsupervised applications. The multiplicative method (or after simple adjustment) can yield acceptable results. These two methods are considered as obsolete, and their performance may be underestimated due to many advanced pan-sharpening techniques being developed recently. Their major advantages include low computational complexity and easy implementation for real-time processing. We believe it is necessary to consider the tradeoff between computational complexity, actual improvement on application, and hardware implementation when developing a pan-sharpening method.

REFERENCES

[1] Y. Zhang, "Understanding image fusion," *Photogramm. Eng. Remote Sens.*, vol. 70, no. 6, pp. 657–661, 2004.

[2] A. Garzelli, F. Nencini, L. Alparone, B. Aiazzi, and S. Baronti, "Pan-sharpening of multispectral image: A critical review and comparison," in *Proc. IGARSS*, 2004, vol. 1, pp. 81–84.

[3] R. Haydan, G. W. Dalke, J. Henkel, and J. E. Bare, "Applications of the IHS colour transform to the processing of multisensor data and image enhancement," in *Proc. Int. Symp. Remote Sens. Arid and Semi-Arid Lands*, Cairo, Egypt, 1982, pp. 599–616.

[4] T.-M. Tu, P. S. Huang, C.-L. Hung, and C.-P. Chang, "A fast intensity–hue–saturation fusion technique with spectral adjustment for IKONOS imagery," *IEEE Geosci. Remote Sens. Lett.*, vol. 1, no. 4, pp. 309–312, Oct. 2004.

[5] V. K. Shettigara, "A generalized component substitution technique for spatial enhancement of multispectral images using a higher resolution data set," *Photogramm. Eng. Remote Sens.*, vol. 58, no. 5, pp. 561–567, 1992.

[6] A. R. Gillespie, A. B. Kahle, and R. E. Walker, "Color enhancement of highly correlated images—II. Channel ratio and 'chromaticity' transformation techniques," *Remote Sens. Environ.*, vol. 22, no. 3, pp. 343–365, 1987.

[7] C. Pohl and J. L. Van Genderen, "Multisensor image fusion in remote sensing: Concepts, methods, and applications," *Int. J. Remote Sens.*, vol. 19, no. 5, pp. 823–854, 1998.

[8] C. A. Laben and B. V. Brower, "Process for enhancing the spatial resolution of multispectral imagery using pan-sharpening," U.S. Patent 6 011 875, U.S. Pat. Off., Washington, DC, Jan. 4, 2000.

[9] Z. Wang, D. Ziou, C. Armenakis, D. Li, and Q. Li, "A comparative analysis of image fusion methods," *IEEE Trans. Geosci. Remote Sens.*, vol. 43, no. 6, pp. 1391–1402, Jun. 2005.

[10] V. Meenakshisundaram, "Quality assessment of IKONOS and QuickBird fused images for urban mapping," M.S. thesis, Univ. Calgary, Calgary, AB, Canada, 2005.

[11] V. Vijayaraj, N. H. Younan, and C. G. O'hara, "Quantitative analysis of pansharpened images," *Opt. Eng.*, vol. 45, no. 4, pp. 046 202-1–046 202-12, 2006.

[12] T. Ranchin and L. Wald, "Fusion of high spatial and spectral resolution images: The ARSIS concept and its implementation," *Photogramm. Eng. Remote Sens.*, vol. 66, no. 1, pp. 49–61, 2000.

[13] R. H. Yuhas, A. F. H. Goetz, and J. W. Boardman, "Discrimination among semi-arid landscape endmembers using the spectral angle mapper (SAM) algorithm," in *Proc. Summaries 3rd Annu. JPL Airborne Geosci. Workshop*, 1992, pp. 147–149.

[14] L. Wald, T. Ranchin, and M. Mangolini, "Fusion of satellite images of different spatial resolutions: Assessing the quality of resulting images," *Photogramm. Eng. Remote Sens.*, vol. 63, no. 6, pp. 691–699, 1997.

[15] Z. Wang and A. C. Bovik, "A universal image quality index," *IEEE Signal Process. Lett.*, vol. 9, no. 3, pp. 81–84, Mar. 2002.

[16] L. Alparone, S. Baronti, A. Garzelli, and F. Nencini, "A global quality measurement of pan-sharpened multispectral imagery," *IEEE Geosci. Remote Sens. Lett.*, vol. 1, no. 4, pp. 313–317, Oct. 2004.

[17] D. Heinz and C.-I Chang, "Fully constrained least squares linear mixture analysis for material quantification in hyperspectral imagery," *IEEE Trans. Geosci. Remote Sens.*, vol. 39, no. 3, pp. 529–545, Mar. 2001.

[18] I. S. Reed and X. Yu, "Adaptive multiple-band CFAR detection of an optical pattern with unknown spectral distribution," *IEEE Trans. Acoust., Speech, Signal Process.*, vol. 38, no. 10, pp. 1760–1770, Oct. 1990.

[19] J. C. Harsanyi, "Detection and classification of subpixel spectral signatures in hyperspectral image sequences," Ph.D. dissertation, Univ. Maryland Baltimore County, Baltimore, MD, 1993.

[20] A. Hyvarinen, "Fast and robust fixed-point algorithms for independent component analysis," *IEEE Trans. Neural Netw.*, vol. 10, no. 3, pp. 626–634, May 1999.